1 Receiver

1.4 MULTIUSER MIMO CHANNEL EQUALIZATION

Christoph F. Mecklenbräuker[†], Joachim Wehinger[†], Thomas Zemen[†], Harold Artés[‡], and Franz Hlawatsch[‡]

In MIMO receivers, the channel state needs to be estimated for equalization, detection, and for feedback to the transmitter in case of adaptive modulation and coding.   Most current iterative [7, 16, 27] and non-iterative [25] schemes in the single-user MIMO case are training-based and rely on the transmission of pilot symbols. Alternatives to pilot-based algorithms are semi-blind schemes which exploit e.g. the known structure of the space-time code to allow reliable channel estimation during ongoing data transmission [2, 3, 18, 20]. Channel estimation and equalization for multiuser MIMO systems involve both information-theoretic [5, 17] and signal processing aspects.

Early contributions to the field of MIMO communications assumed that the receiver has perfect channel state information. Recently there has been increased interest in the case where neither the receiver nor the transmitter know the channel state [11–13, 26]. We consider this case in Section 1.4.2. In [2], a linear space-time modulation technique was proposed which allows the receiver to jointly estimate the channel and demodulate the data without prior channel knowledge at the transmitter or receiver. In Section 1.4.2, this modulation scheme is extended to the case of multiple users.

Section 1.4.3 investigates iterative equalization, detection, and interference cancellation for CDMA with random spreading. An iterative space-time receiver is considered for the uplink of a coded CDMA system. This type of receiver was studied in [1, 19, 29] for perfect channel knowledge. The extension to multipath fading channels incorporating soft decisions for improved

estimation was presented in [30]. We show that such multiuser MIMO communication systems achieve low bit error rates at moderate complexity.

Section 1.4.4 treats equalization of time-variant MIMO multipath channels. We propose a multiuser MIMO equalizer for OFDM using a basis expansion [21, 22] with prolate spheroidal sequences to represent the time-variant mobile radio channel. The resulting block-wise estimator-equalizer fits well to OFDM receiver architectures [31, 34].

1.4.1   Signal and System Model

We consider the multiuser MIMO signal and system model for K simultaneous users shown in Fig. 1.1. In this model, the nth received sample at the qth receiver antenna element is described by

$$r_q[n] = \sum_{k=1}^{K} \sum_{p=1}^{N_\mathrm{T}} \sum_{\ell=0}^{L-1} h_{k,p,q}[n,\ell] b_{k,p}[n-\ell] + v_q[n] \ . \tag{1.1}$$

The (generally time-variant) equivalent baseband MIMO channel impulse response for the kth user is denoted by $h_{k,p,q}[n,\ell]$. Here, $p = 1, \ldots, N_\mathrm{T}$ and $q = 1, \ldots, N_\mathrm{R}$ index the transmit and receive antenna element, respectively. The time sample is denoted by n and ℓ is the delay index. The pth antenna element of the kth user transmits the waveform $b_{k,p}[n]$ at sample time denoted by n. The circular complex zero-mean Gaussian noise with variance σ_v^2 is denoted by $v_q[n]$. In matrix-vector notation, Eq. (1.1) is rewritten as

$$\boldsymbol{r}[n] = \sum_{k=1}^{K} \sum_{\ell=0}^{L-1} \boldsymbol{H}_k[n,\ell] \boldsymbol{b}_k[n-\ell] + \boldsymbol{v}[n] \ , \tag{1.2}$$

where the receive vector $\boldsymbol{r}[n]$ and noise vector $\boldsymbol{v}[n]$ have N_R elements each, $\boldsymbol{H}_k[n,\ell]$ is the $N_\mathrm{R} \times N_\mathrm{T}$ MIMO channel impulse response matrix at sample n and lag ℓ, and the transmit sample vector $\boldsymbol{b}_k[n]$ has N_T elements.

1.4.2   Space-Time Matrix Modulation and Demodulation

A linear *space-time matrix modulation* technique was proposed in [2] allowing the receiver to jointly estimate the channel and demodulate the data. Prior channel state knowledge is neither required at the transmitter nor the receiver. Here, we extend space-time matrix modulation to multiple users. This extension is enabled by a close analogy between the rank-deficient single-user case and the multiuser case [3].

Review of Single-User Space-Time Matrix Modulation.   First, we briefly review space-time matrix modulation for the single-user case. The single-user transmission system is shown in Figure 1.1(b). We consider $N_d <$
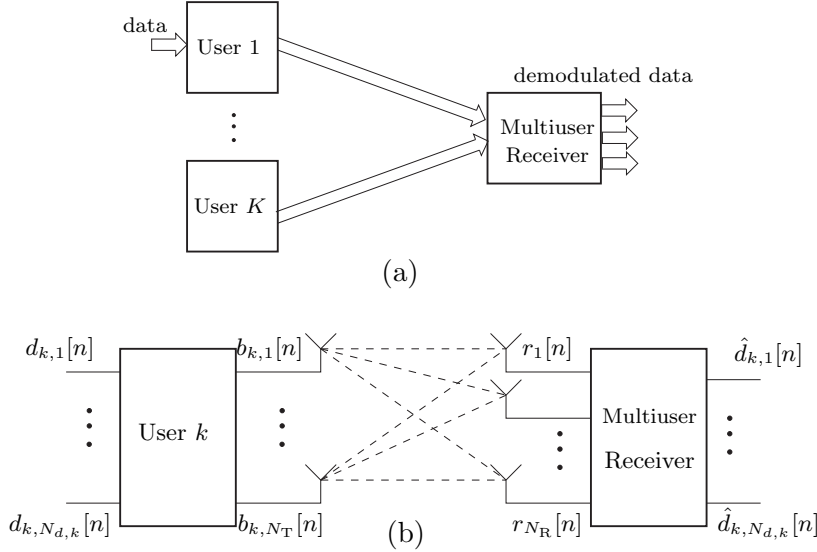
Fig. 1.1   (a) Multiuser MIMO system model, (b) detail for user k.

N_T input data streams $d_1[n], \cdots, d_{N_d}[n]$ with $d_l[n] \in \mathbb{C}$ (i.e., no finite-alphabet assumption is made), where n is the symbol time index. The modulator generates the transmit signal vectors $\boldsymbol{b}[n]$ of dimension N_T according to

$$\boldsymbol{b}[n] \;=\; \sum_{l=1}^{N_d} d_l[n]\,\boldsymbol{m}_l[n]\,, \qquad n = 0, \ldots, M-1\,, \tag{1.3}$$

where M is the block length and the $\boldsymbol{m}_l[n]$ are fixed sequences of *modulation vectors*. Equivalently, we have

$$\boldsymbol{B} \;=\; \sum_{l=1}^{N_d} \boldsymbol{M}_l \boldsymbol{D}_l\,, \tag{1.4}$$

with the $N_\text{T} \times M$ transmit signal matrix $\boldsymbol{B} \triangleq [\boldsymbol{b}[0] \cdots \boldsymbol{b}[M-1]]$, the $N_\text{T} \times M$ *modulation matrices* $\boldsymbol{M}_l \triangleq [\boldsymbol{m}_l[0] \cdots \boldsymbol{m}_l[M-1]]$, and the diagonal $M \times M$ data matrices $\boldsymbol{D}_l \triangleq \text{diag}\{d_l[0], \ldots, d_l[M-1]\}$, where $l = 1, \ldots, N_d$. The modulation vectors $\boldsymbol{m}_l[n]$ (or modulation matrices $\boldsymbol{M}_l$) determine how the data is mapped to the N_T transmit antennas; they are known to the receiver.

   For simplicity of exposition, we assume noiseless transmission (however, in our simulation study in the current Section 1.4.2 we will use a noisy channel). For a single-user, flat-fading, noiseless MIMO channel, (1.2) simplifies to

$$\boldsymbol{r}[n] \;=\; \boldsymbol{H}\,\boldsymbol{b}[n]\,. \tag{1.5}$$

Defining $\boldsymbol{R} \triangleq [\boldsymbol{r}[0] \cdots \boldsymbol{r}[M-1]]$ and inserting (1.4) into (1.5), we obtain

$$\boldsymbol{R} = \boldsymbol{HB} = \boldsymbol{H} \sum_{l=1}^{N_d} \boldsymbol{M}_l \boldsymbol{D}_l \,. \qquad (1.6)$$

From the received matrix $\boldsymbol{R}$, the receiver jointly estimates the data $d_l[n]$ and the unknown channel $\boldsymbol{H}$.

A set of modulation matrices $\{\boldsymbol{M}_1, \cdots, \boldsymbol{M}_{N_d}\}$ will be called *admissible* if the data sequences $d_l[n]$ can be uniquely reconstructed (up to a single constant factor) from the received matrix $\boldsymbol{R}$, without knowledge of $\boldsymbol{H}$. In [2], we showed that for a sufficiently large block length (typically, $M \geq \left\lceil \frac{N_T^2 - 1}{\text{rank}\{\boldsymbol{H}\} - N_d} \right\rceil$), an admissible set of modulation matrices exists if $N_R \geq N_T$ and $\text{rank}\{\boldsymbol{H}\} = N_T$, and we proposed an efficient iterative demodulation algorithm for that case. Indeed, for $N_d < N_T$ as assumed above, the structure enforced by (1.4) corresponds to a *redundancy* of the transmit matrix $\boldsymbol{B}$ which constrains the reconstructed data such that unique reconstruction is possible.

Multiuser Space-Time Matrix Modulation. We now consider the multiuser case as illustrated in Fig. 1.1. There are K users, each of them equipped with N_T transmit antennas and transmitting simultaneously to a single receiver with N_R receive antennas. The kth user has $N_{d,k}$ input data streams $d_{k,l}[n]$ with associated $M \times M$ diagonal data matrices $\boldsymbol{D}_{k,l} \triangleq \text{diag}\{d_{k,l}[0], \ldots, d_{k,l}[M-1]\}$. By a natural extension of our space-time matrix modulation format (1.4), we construct the transmit matrix of the kth user as

$$\boldsymbol{B}_k = \sum_{l=1}^{N_{d,k}} \boldsymbol{M}_{k,l} \boldsymbol{D}_{k,l}, \qquad (1.7)$$

with $N_{d,k}$ modulation matrices $\boldsymbol{M}_{k,l}$ of size $N_T \times M$. The input-output relation of the multiuser channel is

$$\boldsymbol{R} = \sum_{k=1}^{K} \boldsymbol{H}_k \boldsymbol{B}_k, \qquad (1.8)$$

where $\boldsymbol{H}_k$ and $\boldsymbol{B}_k$ are the (unknown) $N_R \times N_T$ channel matrix and the $N_T \times M$ transmit matrix, respectively, associated with the kth user. Inserting (1.7) in (1.8), we obtain the overall input-output relation (which extends (1.6))

$$\boldsymbol{R} = \sum_{k=1}^{K} \boldsymbol{H}_k \sum_{l=1}^{N_{d,k}} \boldsymbol{M}_{k,l} \boldsymbol{D}_{k,l}. \qquad (1.9)$$

We now reformulate this input-output relation for showing the similarity of the multiuser case to the rank-deficient single-user case. Let $\boldsymbol{\mathcal{H}} \triangleq [\boldsymbol{H}_1 \cdots \boldsymbol{H}_K]$

denote the overall channel matrix obtained by stacking the individual channel matrices of all users. Furthermore, let $\boldsymbol{\mathcal{M}}_{k,l} \triangleq \left[\mathbf{0}^{\mathrm{T}} \cdots \mathbf{0}^{\mathrm{T}} \, \boldsymbol{M}_{k,l}^{\mathrm{T}} \, \mathbf{0}^{\mathrm{T}} \cdots \mathbf{0}^{\mathrm{T}} \right]^{\mathrm{T}}$ denote a "zero-padded" modulation matrix of size $KN_{\mathrm{T}} \times M$ that is obtained by stacking $k-1$ zero matrices $\mathbf{0}$ of size $N_{\mathrm{T}} \times M$ above $\boldsymbol{M}_{k,l}$ and $K-k$ such zero matrices below $\boldsymbol{M}_{k,l}$. We rewrite (1.9) as

$$\boldsymbol{R} \,=\, \boldsymbol{\mathcal{H}}\boldsymbol{\mathcal{B}} \,=\, \boldsymbol{\mathcal{H}}\sum_{k=1}^{K}\sum_{l=1}^{N_{d,k}} \boldsymbol{\mathcal{M}}_{k,l}\boldsymbol{D}_{k,l}, \tag{1.10}$$

with $\boldsymbol{\mathcal{B}} \triangleq \sum_{k=1}^{K}\sum_{l=1}^{N_{d,k}} \boldsymbol{\mathcal{M}}_{k,l}\boldsymbol{D}_{k,l}$. Comparing with (1.6), we see that the multiuser case is equivalent to the single-user case with KN_{T} transmit antennas, N_{R} receive antennas, $N_K \triangleq \sum_{k=1}^{K} N_{d,k}$ data streams, a channel matrix $\boldsymbol{\mathcal{H}}$ of size $N_{\mathrm{R}} \times KN_{\mathrm{T}}$, and modulation matrices $\boldsymbol{\mathcal{M}}_{k,l}$ of size $KN_{\mathrm{T}} \times M$ that are nonzero only in the N_{T} rows with indices $kN_{\mathrm{T}} + 1, \ldots, (k+1)N_{\mathrm{T}}$. Typically, there will be $N_{\mathrm{R}} < KN_{\mathrm{T}}$ and thus rank$\{\boldsymbol{\mathcal{H}}\} < KN_{\mathrm{T}}$ (rank-deficient case).

Unique Reconstruction and Flexible User Allocation.   Based on the formulation above, we can use a theorem on identifiability or unique reconstruction for rank-deficient channels [3] to prove the following statements.

Let $N_K < \mathrm{rank}\{\boldsymbol{\mathcal{H}}\}$ and $N_{d,k} < \mathrm{rank}\{\boldsymbol{H}_k\}$, i.e., the total number of data streams is smaller than the rank of the composite channel and the number of data streams transmitted by any user k is smaller than the rank of that user's channel. Furthermore, assume that the block length is large enough (typically, $M \geq \left\lceil \frac{(KN_{\mathrm{T}})^2 - K}{\mathrm{rank}\{\boldsymbol{\mathcal{H}}\} - N_K} \right\rceil$ is sufficient but larger block lengths are advisable for faster convergence of the iterative demodulation algorithm to be proposed below). Then there exist sets of admissible modulation matrices $\boldsymbol{M}_{k,l}$ allowing unique reconstruction of all data streams up to a single unknown constant factor $c_k \in \mathbb{C}$ per user.

Moreover, a set of modulation matrices $\{\boldsymbol{M}_{k,l}\}$ with $k = 1, \cdots, K$ and $l = 1, \cdots, N_{d,k}$ that is admissible in the above setting is also admissible for any single $N_{\mathrm{R}} \times N_{\mathrm{T}}$ matrix $\boldsymbol{H}$ (provided that rank$\{\boldsymbol{H}\}$ is sufficient for the N_K data streams), and the same is true for an arbitrary subset of $\{\boldsymbol{M}_{k,l}\}$. The latter result provides the basis for a flexible multiple-access scheme. Indeed, it means that the modulation matrices of a given admissible set $\{\boldsymbol{M}_{k,l}\}$ can be arbitrarily assigned to the individual users according to their respective data-rate requirements. In the extreme case, all N_K modulation matrices $\boldsymbol{M}_{k,l}$ could be allocated to a single user.

Iterative Blind Demodulation Algorithm.   Given a received matrix $\boldsymbol{R} = \boldsymbol{\mathcal{H}}\boldsymbol{\mathcal{B}}$ and assuming admissible modulation matrices $\boldsymbol{\mathcal{M}}_{k,l}$, our identifiability result implies the following: If the receiver is able to find matrices $\hat{\boldsymbol{\mathcal{H}}}$ and $\hat{\boldsymbol{\mathcal{B}}}$ that satisfy the two properties

1. $\hat{\boldsymbol{\mathcal{H}}}\hat{\boldsymbol{\mathcal{B}}} = \boldsymbol{R}$

2. $\hat{\boldsymbol{\mathcal{B}}} = \sum_{k=1}^{K} \sum_{l=1}^{N_{d,k}} \boldsymbol{\mathcal{M}}_{k,l} \hat{\boldsymbol{D}}_{k,l}$ with $\hat{\boldsymbol{D}}_{k,l}$ diagonal,

then the $\hat{\boldsymbol{D}}_{k,l}$ contain the correct data up to a single constant factor $c_k \in \mathbb{C}$ per user. This motivates an iterative blind demodulation algorithm that is primarily suited for the uplink of a multiuser wireless system because it yields the signals of all users. The ith iteration executes the following two steps.

Step 1 aims at enforcing Property 1. That is, given $\hat{\boldsymbol{\mathcal{B}}}_2^{(i-1)}$ as a result of Step 2 of the previous iteration (see below), we wish to find $\hat{\boldsymbol{\mathcal{H}}}^{(i)}$ and $\hat{\boldsymbol{\mathcal{B}}}_1^{(i)}$ such that $\hat{\boldsymbol{\mathcal{H}}}^{(i)} \hat{\boldsymbol{\mathcal{B}}}_1^{(i)}$ best approximates $\boldsymbol{R}$.

As a first substep, we calculate $\hat{\boldsymbol{\mathcal{H}}}^{(i)}$ such that $\hat{\boldsymbol{\mathcal{H}}}^{(i)} \hat{\boldsymbol{\mathcal{B}}}_2^{(i-1)}$ best approximates $\boldsymbol{R}$ in the least-squares (LS) sense. This gives $\hat{\boldsymbol{\mathcal{H}}}^{(i)} = \boldsymbol{R} \hat{\boldsymbol{\mathcal{B}}}_2^{(i-1)\#}$, where $\hat{\boldsymbol{\mathcal{B}}}_2^{(i-1)\#}$ denotes the pseudo-inverse of $\hat{\boldsymbol{\mathcal{B}}}_2^{(i-1)}$. As a second substep, we calculate $\hat{\boldsymbol{\mathcal{B}}}_1^{(i)}$ such that $\hat{\boldsymbol{\mathcal{H}}}^{(i)} \hat{\boldsymbol{\mathcal{B}}}_1^{(i)}$ best approximates $\boldsymbol{R}$ in the LS sense. This gives the final result

$$\hat{\boldsymbol{\mathcal{B}}}_1^{(i)} = \hat{\boldsymbol{\mathcal{H}}}^{(i)\#} \boldsymbol{R} = \left(\boldsymbol{R} \hat{\boldsymbol{\mathcal{B}}}_2^{(i-1)\#}\right)^{\#} \boldsymbol{R}. \tag{1.11}$$

Step 2 enforces Property 2. That is, we approximate $\hat{\boldsymbol{\mathcal{B}}}_1^{(i)}$ from Step 1 above by a matrix $\hat{\boldsymbol{\mathcal{B}}}_2^{(i)}$ with the modulation structure of Property 2, i.e., $\hat{\boldsymbol{\mathcal{B}}}_2^{(i)} = \sum_{k=1}^{K} \sum_{l=1}^{N_{d,k}} \boldsymbol{\mathcal{M}}_{k,l} \hat{\boldsymbol{D}}_{k,l}^{(i)}$. The diagonal matrices $\hat{\boldsymbol{D}}_{k,l}^{(i)}$ are chosen such that $\hat{\boldsymbol{\mathcal{B}}}_2^{(i)}$ best approximates $\hat{\boldsymbol{\mathcal{B}}}_1^{(i)}$ in the LS sense. It can be shown that the nonzero (diagonal) elements of $\hat{\boldsymbol{D}}_{k,l}^{(i)}$ are given by

$$\left(\hat{\boldsymbol{D}}_{k,l}^{(i)}\right)_{n,n} = \frac{1}{N_{\mathrm{T}}} \sum_{j=1}^{N_{\mathrm{T}}} \left(\hat{\boldsymbol{\mathcal{B}}}_1^{(i)}\right)_{j,n} \left(\mathbf{C}_{\lambda(k,l)}^{(i)}\right)_{j,n} \quad \text{with } \lambda(k,l) \triangleq \sum_{\kappa=1}^{k-1} N_{d,\kappa} + l, \tag{1.12}$$

where the $\mathbf{C}_{\lambda}^{(i)}$ are matrices of size $N_{\mathrm{T}} \times M$ that are constructed as follows. Let $\boldsymbol{\mu}_{k,l}[n]$ with $n = 0, \ldots, M-1$ denote the $(n+1)$th column of $\boldsymbol{\mathcal{M}}_{k,l}$, i.e., $\boldsymbol{\mathcal{M}}_{k,l} = \left[\boldsymbol{\mu}_{k,l}[0] \cdots \boldsymbol{\mu}_{k,l}[M-1]\right]$. Furthermore, for fixed n, let $\boldsymbol{M}[n]$ denote the $N_{\mathrm{T}} \times N_K$ matrix that contains the nth columns of all $\boldsymbol{\mathcal{M}}_{k,l}$ for $l = 1, \ldots, N_{d,k}$ and $k = 1, \ldots, K$, i.e.,

$$\boldsymbol{M}[n] \triangleq \left[\boldsymbol{\mu}_{1,1}[n] \cdots \boldsymbol{\mu}_{1,N_{d,1}}[n] \ \cdots \ \boldsymbol{\mu}_{K,1}[n] \cdots \boldsymbol{\mu}_{K,N_{d,K}}[n]\right]. \tag{1.13}$$

Then, the nth column of $\mathbf{C}_{\lambda}^{(i)}$ is defined as the λth row of the $N_K \times N_{\mathrm{T}}$ matrix $\left(\hat{\boldsymbol{\mathcal{H}}}^{(i)\#} \hat{\boldsymbol{\mathcal{H}}}^{(i)} \boldsymbol{M}[n]\right)^{\#}$, where $\hat{\boldsymbol{\mathcal{H}}}^{(i)}$ was calculated in Step 1 above.

This algorithm yields an estimate $\hat{\boldsymbol{\mathcal{H}}}^{(i)}$ of the channel matrix in Step 1 and estimates $\hat{\boldsymbol{D}}_{k,l}^{(i)}$ of the data matrices in Step 2. In the noise-free case, we always observed the algorithm to converge to the correct channel and data matrices up to a single complex factor per user. Results in the presence of noise will be shown next.
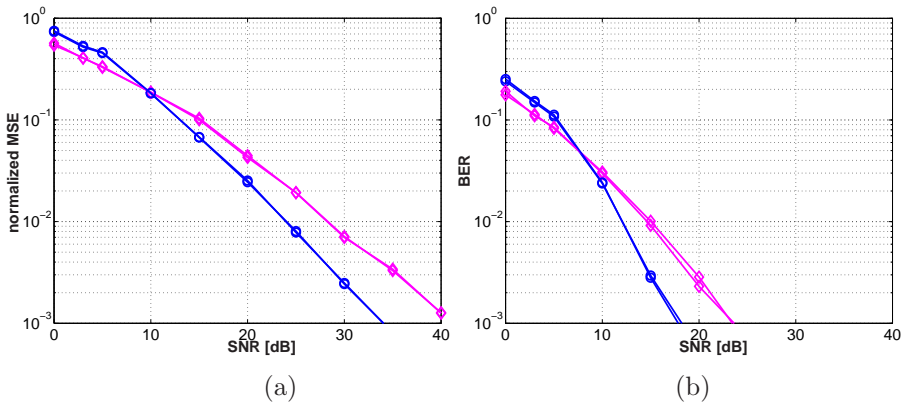
Fig. 1.2   (a) Normalized MSE vs. SNR obtained with space-time matrix modulation using the iterative demodulation algorithm. (b) corresponding BER vs. SNR. ◇——◇: Single-user case—two data streams assigned to a single user; ○——○: multiuser case—one data stream assigned to each of two different users.

Simulation Results and Discussion.   We carried out both a single-user experiment and a multiuser experiment, in which we transmitted i.i.d. complex Gaussian signals $d_{k,l}[n] \in \mathbb{C}$ over channels with $N_\mathrm{T} = 4$ transmit antennas and $N_\mathrm{R} = 4$ receive antennas. The modulation matrices $\boldsymbol{\mathcal{M}}_{k,l}$ with block length $M = 100$ were constructed by taking realizations of i.i.d. Gaussian random variables as matrix entries and then orthonormalizing the corresponding columns of all $\boldsymbol{\mathcal{M}}_{k,l}$ (in our simulations, this always resulted in admissible modulation matrices). The channels were randomly generated for each simulation run. The channel output signals were corrupted by white Gaussian noise.

In the single-user case, we transmitted $N_d = 2$ data streams. In the multiuser case, we considered $K = 2$ users with one data stream each (thus, $N_K = 2$). Fig. 1.2a shows the total normalized mean-square error (MSE) of the data streams reconstructed by means of our iterative blind demodulation algorithm versus the signal-to-noise ratio (SNR). We see that for high SNR, the MSE is significantly smaller when the data streams are assigned to different users than when one user transmits all data streams.

We discuss this result in the following. In the multiuser case, there are eight transmit antennas (four per user) against four in the single-user case. Thus, even though the individual users do not cooperate, the multiuser channel offers more diversity than the single-user channel. The results show that the iterative blind demodulation algorithm exploits some of this extra diversity in the multiuser case. Note that we have not exploited channel knowledge, neither at the transmitter nor at the receiver. In the multiuser case, we have to estimate twice as many unknown channel parameters as in the single-user case.

Finally, Fig. 1.2b shows the corresponding bit error rate (BER) versus the SNR when a 4-QAM transmit alphabet is used instead of the Gaussian source. The iterative demodulation algorithm is followed by a quantization to the 4-QAM alphabet. The BERs decrease more rapidly than the corresponding normalized MSEs.

Space-time matrix modulation allows to transmit data streams from multiple users over *unknown* MIMO channels. An efficient iterative receiver algorithm is proposed which exploits the modulation structure to jointly estimate data and channels for multiple users. Unique demodulation in the noise-free case is guaranteed theoretically. Simulations demonstrate good performance of the proposed space-time matrix modulation/demodulation in the presence of noise.

1.4.3   Iterative Space-Time Equalization and Demodulation for Coded CDMA

An iterative receiver with space-time processing is considered for the uplink of a coded CDMA system. We assume that symbols are transmitted synchronously and multipath propagation is modelled with a temporal granularity of a chip duration. The receiver consists of a multiuser detector, a bank of single-user decoders, and a channel estimator, see Fig. 1.3. The behavior of iterative receivers which employ ML channel estimation was reported in [14] for the special case of a single propagation path with constant amplitude. The results in this section are obtained for a receiver with N_R antenna elements. We show that such multiuser MIMO communication systems achieve low bit-error rates at moderate complexity.

Signal Model.   We assume that the propagation channel has block-fading characteristic, i.e., the channel is constant over a block of M transmit symbols. Thus, $h_{k,p,q}[n,\ell]$ in the system model (1.1) does not depend on n. The first J symbols are pilots which are used for channel identification at each receiver antenna element. The subsequent $M - J$ symbols are QPSK symbols, derived from an uncoded information bit stream $d_k[m'']$ which is convolutionally encoded, randomly interleaved, and Gray mapped. The resulting M QPSK symbols $a_k[m]$ of user k are spread by the sequence $\boldsymbol{s}_k$ of dimension $N \times 1$. We reformulate (1.1) by separating the single term for $\ell = 0$ from the remaining terms at lags $\ell > 0$,

$$
r_q[n] \;=\; \sum_{k=1}^{K} \Big(h_k[0] a\left[\lfloor n/N \rfloor\right] s_k[n \mod N] \;+
$$
$$
\sum_{\ell=1}^{L-1} h_k[\ell] a\left[\lfloor n/N \rfloor - 1\right] s_k[N - n \mod N] \Big) . \quad (1.14)
$$

(a)

(b)

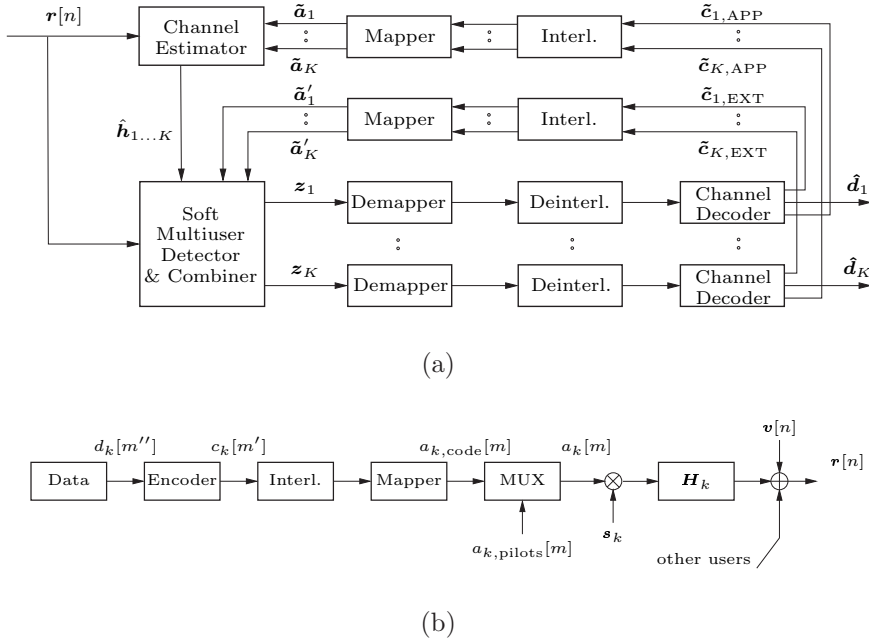**Fig. 1.3**   (a) Iterative multiuser MIMO equalization. (b) Uplink transmitter.

The elements of the sequence s_k are randomly drawn from the set $\{\pm 1 \pm j\}/\sqrt{2N}$ such that $\|s_k\|^2 = 1$. The uplink transmitter is shown in Fig. 1.3b.

The system model (1.1) reflects the superposition of inter-symbol interference (ISI) and multiple-access interference (MAI) components at the chip level n. Here, we assume that each user has a single transmit antenna, $N_T = 1$, and we will thus omit the transmit antenna-element index p in the following. Note that a transmit symbol at time m is spread to a signal of length N. The channel is modelled on the chip level and has L taps such that the total receive vector affected by symbol $a[m]$ is of length $N + L - 1$. We denote this vector as

$$y_q[m] \triangleq [r_q[(m-1)N+1]\ldots r_q[mN+L]]^{\mathrm{T}}. \tag{1.15}$$

Note that $y_q[m]$ describes a vector of temporally successive chip samples for one receive antenna whereas $r[n]$ in (1.1) describes a vector of chip samples at one chip instant but for all receive antennas.

The receiver consists of three processing units exchanging information on code symbols and channel estimates in an iterative manner. We will explain the individual parts in the sequel.

Soft Multiuser Detection.   We implement and investigate multiuser detection with a parallel interference cancelling (PIC) unit and a subsequent single-user matched filter (SUMF) or a linear minimum mean square error

(LMMSE) filter. Parallel interference cancellation is implemented using soft decisions $\tilde{a}'_k[m]$ defined in (1.29). These are obtained from the estimated *extrinsic* probabilities (EXT) of the code symbols available at the output of the channel decoder, see Fig. 1.3a. See the section "Decoding" on page 12 for further details. Soft decisions require the signature sequences to be known, their timing, and an estimate for the channel state. The interference canceller removes MAI. ISI terms are explicitly considered in the cancellation since they can greatly influence the receiver performance when the channel memory length L cannot be considered much smaller than N. If exact knowledge of all interfering users' symbols and the channel state were available, then the MAI could be eliminated perfectly. However, due to inaccurate channel knowledge and errors in the feedback symbols this cannot be achieved. Usually, the process of interchanging information is done iteratively several times. The effective spreading sequence of user k at antenna element q is $\tilde{\boldsymbol{s}}_{k,q} = \boldsymbol{s}_k * \hat{h}_{k,q}$ with $*$ denoting convolution and $\hat{h}_{k,q}$ being a channel estimate. Stacking these vectors together leads to the effective spreading matrix $\tilde{\boldsymbol{S}}_q$ of dimension $(N + L - 1) \times K$. The observation window covers both pre– and postcursor ISI. The ISI length is

$$W = \lceil (N + L - 1)/N \rceil \ . \tag{1.16}$$

The parallel interference canceller (PIC) calculates

$$\tilde{\boldsymbol{y}}_{k,q}[m] = \boldsymbol{y}_q[m] + \tilde{\boldsymbol{s}}_{k,q}\tilde{a}'_k[m] - \sum_{w=-W+1}^{W-1} \tilde{\boldsymbol{S}}_q[w]\tilde{\boldsymbol{a}}'[m - w]. \tag{1.17}$$

Terms indexed by $w > 0$ in the sum above correspond to ISI caused by future symbols while terms indexed by $w < 0$ are related to preceding symbols. The matrices attributed to previous and future symbols are defined by

$$\tilde{\boldsymbol{S}}_q[w] = \begin{cases} \begin{pmatrix} \tilde{s}_{1,q}[wN + 1] & \dots & \tilde{s}_{K,q}[wN + 1] \\ \tilde{s}_{1,q}[wN + 2] & \dots & \tilde{s}_{K,q}[wN + 2] \\ \vdots & \ddots & \vdots \\ \tilde{s}_{1,q}[wN + \Delta] & \dots & \tilde{s}_{K,q}[WN + \Delta] \\ \boldsymbol{0}_{wN} & \dots & \boldsymbol{0}_{wN} \end{pmatrix} & \text{for } w < 0 \\ \\ \tilde{\boldsymbol{S}}_q & \text{for } w = 0 \end{cases} \tag{1.18}$$

with $\Delta = (N + L - 1) - (W - 1)N$ and correspondingly for $w > 0$. After MAI removal, the signal is passed through a linear filter whose output is

$$z_{k,q}[m] = \boldsymbol{f}_{k,q}^{\mathrm{H}}[m]\tilde{\boldsymbol{y}}_{k,q}[m]. \tag{1.19}$$

We focus our interest on the SUMF and LMMSE filter. The latter filter is more involved due to the required matrix inversion. For certain system loads

$\alpha = K/N$, the SUMF achieves the same BER as the LMMSE filter, but requires a higher number of iterations [6]. Results for both filters are shown in Fig. 1.4 on page 15.

The single-user matched filter is

$$\boldsymbol{f}_{k,q}[m] = \tilde{\boldsymbol{s}}_{k,q}[m] \ , \tag{1.20}$$

and the LMMSE filter is defined as

$$\boldsymbol{g}_{k,q}[m] = \underset{\boldsymbol{g}}{\operatorname{argmin}} \, \mathbb{E} \left\{ \left| a_k[m] - \boldsymbol{g}^{\mathrm{H}} \tilde{\boldsymbol{y}}_{k,q}[m] \right|^2 \right\} . \tag{1.21}$$

A solution to (1.21) is found under the assumption of independent symbols $a_k[m]$ and when known symbols $a_k[m]$ are replaced by their estimates $\tilde{a}'_k[m]$ defined in (1.29). Then the filter becomes

$$\boldsymbol{g}_{k,q}^{\mathrm{H}}[m] = \tilde{\boldsymbol{s}}_{k,q}^{\mathrm{H}}[m] \left(\sigma_v^2 \boldsymbol{I} + \tilde{\boldsymbol{s}}_{k,q}[m] |\tilde{a}'_k[m]|^2 \tilde{\boldsymbol{s}}_{k,q}^{\mathrm{H}}[m] + \sum_{w=-W+1}^{W-1} \tilde{\boldsymbol{S}}_q[w] \boldsymbol{V}[m] \tilde{\boldsymbol{S}}_q^{\mathrm{H}}[w] \right)^{-1} \tag{1.22}$$

with $\boldsymbol{V}[m]$ denoting the diagonal covariance matrix

$$\boldsymbol{V}[m] = \mathbb{E} \left\{ \left(\boldsymbol{a}[m] - \mathbb{E}\{\boldsymbol{a}[m]\} \right) \left(\boldsymbol{a}[m] - \mathbb{E}\{\boldsymbol{a}[m]\} \right)^{\mathrm{H}} \right\} \ . \tag{1.23}$$

Now, we substitute $\mathbb{E}\{\boldsymbol{a}[m]\}$ by the *extrinsic* probability (EXT) $\tilde{\boldsymbol{a}}'[m]$ defined via (1.29). The resulting $\boldsymbol{V}[m]$ has diagonal elements $V_{k,k}[m] = 1 - \mathbb{E}\left\{ |\tilde{a}'_k[m]|^2 \right\}$. When $V_{k,k}[m]$ is computed for each symbol individually, the resulting filter is termed *conditional*. This, however, involves a matrix inversion for each symbol and every user. An alternative approach averages over all code symbols in a single block to construct a $\boldsymbol{V} = \operatorname{diag}(V_{1,1}, \ldots, V_{K,K})$ which does not depend on the symbol index m. In this way, the filter needs to be computed only once for every user and iteration. The resulting filter is called *unconditional* [9].

We have obtained a biased filter so far. The bias is $\beta[m] = \mathbb{E}\{z_{k,q}[m]/a_k[m]\} = \boldsymbol{g}_{k,q}^{\mathrm{H}}[m]\tilde{\boldsymbol{s}}_{k,q}[m]$. An unbiased and unconditional modification of (1.22) is $\boldsymbol{g}'^{\mathrm{H}}_{k,q}[m] = \frac{1}{\beta}\boldsymbol{g}_{k,q}^{\mathrm{H}}[m]$ which results in

$$\boldsymbol{g}'^{\mathrm{H}}_{k,q}[m] = \frac{\tilde{\boldsymbol{s}}_{k,q}^{\mathrm{H}}[m]\boldsymbol{Z}_q^{-1}}{\tilde{\boldsymbol{s}}_{k,q}^{\mathrm{H}}[m]\boldsymbol{Z}_q^{-1}\tilde{\boldsymbol{s}}_{k,q}[m]} \quad \text{with } \boldsymbol{Z}_q = \sum_{w=-W+1}^{W-1} \tilde{\boldsymbol{S}}_q[w]\boldsymbol{V}\tilde{\boldsymbol{S}}_q^{\mathrm{H}}[w] + \sigma_v^2\boldsymbol{I}. \tag{1.24}$$

Antenna Combining.   The unbiased and unconditional LMMSE filter $\boldsymbol{g}'_{k,q}[m]$ is applied to the receive vector. A soft decision is obtained by maximum ratio combining (MRC) of all antennas by using the estimate $\hat{\boldsymbol{h}}_{k,q}$ for the channel

impulse response defined in (1.31),

$$z_k[m] = \sum_{q=1}^{N_{\mathrm{R}}} \|\hat{\boldsymbol{h}}_{k,q}\|^2 \boldsymbol{g}'^{\mathrm{H}}_{k,q} \tilde{\boldsymbol{y}}_{k,q}[m] \bigg/ \sum_{q=1}^{N_{\mathrm{R}}} \|\hat{\boldsymbol{h}}_{k,q}\|^2 \ . \tag{1.25}$$

Decoding. The soft decision feedback supplied to the channel and the data estimator are computed from the *a posteriori* probabilities (APP) and the *extrinsic* probabilities (EXT). A soft input soft output decoder for the binary convolutional code is implemented by the BCJR algorithm [4] which estimates these quantities. The decoder input is given by the channel values $x_k[m']$ which are obtained from the $z_k[m]$ given in (1.25) through sequential de-mapping to a real sequence and de-interleaving (see Fig. 1.3a). They are the received values for the $2(M-J)$ code bits $c_k[m']$. The conditional probability density of the multiuser detector (MUD) output values $x_k[m']$ can be modelled by a Gaussian distribution with mean $\pm\mu$ and variance ν_k^2. The decision-directed estimate for the mean is $\hat{\mu} = 1/(2(M-J)) \sum_{i=1}^{2(M-J)} |x_k[i]|$ and for the variance $\hat{\nu}_k^2 = \frac{1}{2(M-J)} \sum_{i=1}^{2(M-J)} |x_k[i]|^2 - \hat{\mu}$. The APP for having the value $+1$ as code bit when observing the channel value $x_k[m']$ is given as $\mathrm{APP}_k[m'] = \Pr\{c_k[m'] = +1 \mid \boldsymbol{x}_k\}$ where the vector $\boldsymbol{x}_k$ contains all $x_k[m']$ of the code block. The link between the APP and the EXT is established via the relation

$$\mathrm{APP}_k[m'] \propto \mathrm{EXT}_k[m'] \, p\left(x_k[m'] \mid c_k[m'] = 1\right) \tag{1.26}$$

where the last term denotes the channel transition function which is assumed to be a Gaussian probability density in this section, estimated parametrically as

$$p\left(x_k[m'] \mid c_k[m'] = 1\right) \propto \exp(-|x_k[m'] - \hat{\mu}|^2/\hat{\nu}_k^2) \ . \tag{1.27}$$

The APP values are normalized such that $\Pr\{c_k[m'] = +1|\boldsymbol{x}_k\} + \Pr\{c_k[m'] = -1|\boldsymbol{x}_k\} = 1$; the EXT values are normalized in the same way. After interleaving, these probabilities are used to obtain an estimate of the transmitted symbols. The QPSK mapping for the APPs and the EXTs is given by

$$\begin{aligned}
\tilde{a}_k[J+m] &= \left[1 - 2\,\mathrm{APP}_k[2m] + \mathrm{j}(1 - 2\,\mathrm{APP}_k[2m+1])\right]/\sqrt{2} \ , &(1.28)\\
\tilde{a}'_k[J+m] &= \left[1 - 2\,\mathrm{EXT}_k[2m] + \mathrm{j}(1 - 2\,\mathrm{EXT}_k[2m+1])\right]/\sqrt{2} \ , &(1.29)
\end{aligned}$$

with $m \in \{1, \dots, M-J\}$. The symbol estimates $\tilde{a}'_k[m]$ are used in the feedback branch to the detector with PIC and SUMF/LMMSE filtering while the soft decisions $\tilde{a}_k[m]$ are used for channel estimation as if they were additional pilot symbols.

Channel Estimation. In a system with multiple receive antennas, all paths to the receive antennas need to be estimated. The initial estimate is based on

training symbols in the preamble of the block of transmit symbols. In later iterations, the estimator is enhanced by incorporating soft decisions $\tilde{a}_k[m]$ derived from the APPs as described in (1.28).

It was shown in [8] that long spreading sequences with elements taken from the unit circle exhibit nice cross-correlation properties. These sequences are called Perfect Root of Unity Sequences (PRUS) and are particularly well suited for multipath channel estimation with long delay spread. In our receiver, we choose a length of JN.

For channel estimation, we need to estimate each single propagation path and we model the signal somewhat different from (1.1),

$$
\boldsymbol{y}_q = \left(\sum_{w=1}^{W} \boldsymbol{\mathcal{D}}_w \boldsymbol{\mathcal{A}}_w \right) \boldsymbol{h}_q + \boldsymbol{v}_q = \boldsymbol{\mathcal{U}} \boldsymbol{h}_q + \boldsymbol{v}_q \;, \tag{1.30}
$$

where the various quantities involved are described below.   The $MN \times 1$ vector $\boldsymbol{y}_q$ contains samples at the chiprate received at antenna q.   The $MN \times MKL$ matrix $\boldsymbol{\mathcal{D}}_w$ is block diagonal and defined as $\mathrm{diag}(\underbrace{\boldsymbol{D}_w \ldots \boldsymbol{D}_w}_{M})$, where $\boldsymbol{D}_w = [\boldsymbol{D}_{w,1} \ldots \boldsymbol{D}_{w,K}]$ is of dimension $N \times KL$. The matrix $\boldsymbol{D}_{w,k}$ is derived from the $WN \times L$ matrix

$$
\boldsymbol{C}_k = \left(
\begin{array}{cccccccc}
s_k[1] & & & & & & & \\
s_k[2] & s_k[1] & & & & & & \\
s_k[3] & s_k[2] & s_k[1] & & & & & \\
\vdots & \vdots & \ddots & \ddots & & & & \\
s_k[N] & s_k[N-1] & s_k[N-2] & \ldots & s_k[1] & & & \\
& s_k[N] & s_k[N-1] & \ldots & s_k[2] & s_k[1] & & \\
& & s_k[N] & \ldots & s_k[3] & s_k[2] & \ddots & \\
& & & \ddots & \vdots & \vdots & \vdots & \\
& & & & & s_k[N] & & \vdots \\
& & & & & & s_k[N] & \ddots \\
& & & & & & \vdots & \ddots
\end{array}
\right) .
$$

Elements which are not covered by the shifted spreading sequence are zero. The matrix $\boldsymbol{D}_{w,k}$ contains the rows from $(w-1)N + 1$ to wN of $\boldsymbol{C}_k$. An exception is the construction of the first J matrices $\boldsymbol{D}_w$ for which the corresponding PRUSs are taken instead of the vectors $\boldsymbol{s}_k$. $\boldsymbol{\mathcal{A}}_{\boldsymbol{w}} = [\boldsymbol{A}[1-w] \boldsymbol{A}[2-w] \ldots \boldsymbol{A}[M-w]]^{\mathrm{T}}$ is an $MKL \times KL$ vertically stacked matrix consisting of the diagonal $KL \times KL$ matrices

$$
\boldsymbol{A}[m] = \mathrm{diag}\left(\boldsymbol{a}_1[m] \; \boldsymbol{a}_2[m] \ldots \boldsymbol{a}_K[m] \right) \qquad \text{with} \;\; \boldsymbol{a}_k[m] = \tilde{a}_k[m] \boldsymbol{1}_L \; .
$$

$\boldsymbol{h}_q$ is a $KL \times 1$ vector obtained by vertically stacking the $L \times 1$ chip impulse responses $\boldsymbol{h}_{k,q}$ of all users' channels, i.e. $\boldsymbol{h}_q = \left[\boldsymbol{h}_{1,q}^{\mathrm{T}} \ \boldsymbol{h}_{2,q}^{\mathrm{T}} \dots \ \boldsymbol{h}_{K,q}^{\mathrm{T}}\right]^{\mathrm{T}}$. Finally, $\boldsymbol{v}_q$ designates an $NM \times 1$ zero-mean complex Gaussian noise vector with covariance matrix $\sigma_v^2 \boldsymbol{I}_{NM}$. A least squares (LS) estimator of $\boldsymbol{h}_q$ requires the symbols to be *known*. We replace the symbols $a_k[m]$ by their soft decisions $\tilde{a}_k[m]$ from (1.28). Using $\boldsymbol{\mathcal{U}}$ introduced in (1.30), we obtain the estimate

$$\hat{\boldsymbol{h}}_q = (\boldsymbol{\mathcal{U}}^{\mathrm{H}}\boldsymbol{\mathcal{U}})^{-1}\boldsymbol{\mathcal{U}}^{\mathrm{H}}\boldsymbol{y}_q \ . \tag{1.31}$$

Simulation Results and Discussion. For illustration of the iterative space-time receiver concept, we use spreading factor $N = 16$. The encoder is a non-systematic, non-recursive convolutional code with rate $C_R = 1/2$ and generator polynomials $(5,7)_8$. The channel estimator uses the approximated LS approach formulated in (1.31). We assume an i.i.d. Rayleigh fading channel model with a delay spread L of 5 chips. The taps are normalized such that $\mathbb{E}\left\{\sum_{q=1}^{N_{\mathrm{R}}} \sum_{\ell=0}^{L-1} |h_{k,q}[\ell]|^2\right\} = 1$. We consider the channel impulse response to be constant during the transmission of a code block. The block length is $M = 250$ symbols out of which $J = 20$ are pilots which corresponds to $8\,\%$ of the transmitted energy. To account for the energy loss due to the pilots we define the ratio of energy per information bit and noise power spectral density as $E_b/N_0 = \frac{1}{\sigma_v^2 C_R}\frac{M}{M-J}$.

In Fig. 1.4, the BER vs. E_b/N_0 is shown for the PIC detectors with the SUMF and the LMMSE filter. The plot compares the difference in BER of the two detectors as well as the impact of using soft decisions to support the channel estimator. For the moment, we consider single-antenna reception in an overloaded system with load $\alpha = K/N = 1.5$. We illustrate the BER after the first, third, and sixth iterations together with single-user-bound (SUB) which is defined as the BER in case of a single user in the system having perfect channel state information. We notice that using feedback symbols in the multiuser detector and the channel estimator allows BER's of 10^{-3} after 6 iterations at an E_b/N_0 of 8.6 dB using a LMMSE filter and at 12.7 dB in case of the SUMF. The gap in E_b/N_0 between the two detectors at a BER of 10^{-3} is 4.1 dB. The LMMSE-based receiver is able to approach the SUB as close as 0.4 dB at an E_b/N_0 of 8 dB after 6 iterations. Furthermore, the results reveal that soft decision feedback for channel estimation improves the receiver performance considerably. When comparing the LMMSE receiver with a channel estimator using soft decision feedback with a receiver which uses pilots only for channel estimation, we observe an improvement of more than 2 dB. This improvement becomes even more pronounced in the SUMF-based receiver where a reasonable BER can not be obtained with just 6 iterations.

Finally, Fig. 1.5 shows the BER versus the number of users K in the one– and two antenna cases. These results were obtained from simulations at an E_b/N_0 of 8 dB. For a single antenna and 10 iterations, the system serves up

to 30 users while operating close to a BER of 10^{-3}. The plot shows that the number of supported users is drastically increased if two receive antennas are used. More users can be accomodated at the cost of an increased number of iterations. With two receive antennas, more than 50 users can be served in simultaneous links with a BER lower than 10^{-3} after 10 iterations. This is enabled by the reduced variability of the receiver-side signal power when employing multiple receive antennas.
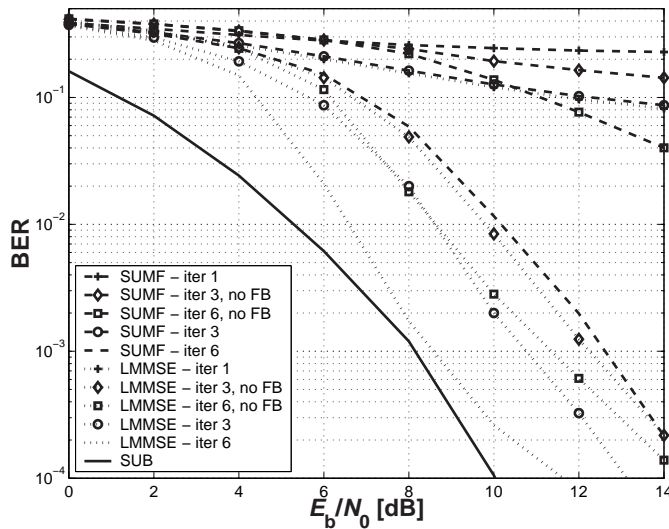
Fig. 1.4   BER vs. E_b/N_0 for the PIC-SUMF and PIC-LMMSE detectors with and without the use of soft decisions for channel estimation. The parameters are $K = 24$, $N = 16$, $L = 5$, $M = 250$, and $J = 20$.

We have demonstrated that an iterative receiver impressively increases the number of supported users when employing antenna diversity at the base-station receiver. These performance gains are achieved in a multipath environments when soft decision feedback is used for both *channel estimation* and *interference cancellation*.

1.4.4   Basis Expansion for Time-Variant Channel Equalization

This section deals with the equalization of time-variant channels by extending the iterative receiver concept developed in Section 1.4.3 for block-fading channels. The variation of a wireless channel over the duration of a data block is caused by user mobility and multipath propagation. The Doppler shifts on the individual paths depend on the user's velocity v, the carrier frequency f_C, and the scattering environment. The maximum variation in time of the wireless channel is upper bounded by the maximum (one sided) normalized
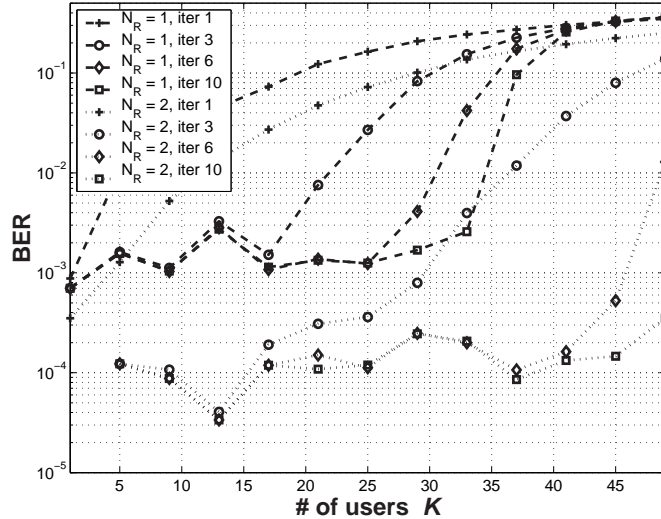
Fig. 1.5 Achievable BER vs. the number of users K for the PIC-LMMSE detector with one and two receive antennas. The parameters are $N = 16$, $L = 5$, $M = 250$, $J = 20$, and $E_b/N_0 = 8\,\mathrm{dB}$.

Doppler bandwidth

$$\nu_{\mathrm{Dmax}} = B_{\mathrm{D}} T_{\mathrm{S}}\,, \tag{1.32}$$

where $B_{\mathrm{D}} = \frac{v_{\max} f_{\mathrm{C}}}{c_0}$ is the maximum Doppler bandwidth, $v_{\max}$ is the maximum velocity, T_{S} is the symbol duration, and c_0 denotes the speed of light.

We apply orthogonal frequency division multiplexing (OFDM) in order to transform the time-variant frequency-selective channel into a set of parallel time-variant frequency-flat channels, the so-called subcarriers. We consider time-variant channels which may vary significantly over the duration of a long block of OFDM symbols. However, for the duration of each single OFDM symbol, the channel variation is assumed small enough to be neglected. This implies a very small inter-carrier interference (ICI). Each OFDM symbol is preceded by a cyclic prefix to avoid inter-symbol interference (ISI).

The discrete-time sequence of channel coefficients for each frequency-flat subcarrier is bandlimited by ν_{Dmax}. It was shown by Slepian [24] that time-limited parts of bandlimited sequences span a low-dimensional subspace. A natural set of basis functions for this subspace is given by the so-called discrete prolate spheroidal sequences. A Slepian basis expansion using this subspace representation was proposed in [31] for time-variant channel equalization. It was shown in [34] that the channel estimation bias obtained with the Slepian basis expansion is more than a magnitude smaller compared to the Fourier basis expansion (i.e. a truncated discrete Fourier transform) [22].

An iterative time-variant channel estimation scheme is developed by combining pilot symbols with soft decisions for estimating the coefficients of the Slepian basis expansion.

MIMO-OFDM Multiuser Signal Model for Doubly Selective Channels. Every user has a single $N_{\mathrm{T}} = 1$ transmit antenna, the base station has N_{R} receive antennas. There are K users. We consider the equalization and detection problem for such a $K \times N_{\mathrm{R}}$ multiuser MIMO communications system. Each user's data symbols are spread over N subcarriers by means of a user-specific spreading code. The transmission is block-oriented; a data block consists of $M - J$ OFDM data symbols and J OFDM pilot symbols.

The data symbols are chosen from a QPSK symbol constellation. The data symbols are given by $a_k[m] \in \{\pm 1 \pm \mathrm{j}\}/\sqrt{2}$ for $m \notin \mathcal{P}$ and $a_k[m] = 0$ for $m \in \mathcal{P}$, where the pilot placement is defined by the index set

$$\mathcal{P} = \{\lfloor M/J(i + 1/2) \rfloor \mid i = 0, \ldots, J - 1\} \tag{1.33}$$

and discrete time at rate $1/T_{\mathrm{S}} = 1/(PT_{\mathrm{C}})$ is denoted by m. After the spreading operation, pilot symbols $\boldsymbol{p}_k[m] \in \mathbb{C}^N$ with elements $p_k[m, e]$ are added, giving the $N \times 1$ vectors

$$\boldsymbol{d}_k[m] = \boldsymbol{s}_k a_k[m] + \boldsymbol{p}_k[m]. \tag{1.34}$$

The elements of the pilot symbols $p_k[m, e]$ for $m \in \mathcal{P}$ and $e \in \{0, \ldots, N - 1\}$ are randomly chosen from the QPSK symbol set $\{\pm 1 \pm \mathrm{j}\}/\sqrt{2N}$. For $m \notin \mathcal{P}$ we define $\boldsymbol{p}_k[m] = \boldsymbol{0}_N$. Subsequently, an N-point inverse discrete Fourier transform (DFT) is carried-out and a cyclic prefix of length G is inserted. An OFDM symbol including the cyclic prefix has length $P = N + G$ chips.

The temporal channel variation for the duration of each single OFDM symbol is small which translates to small ICI [15]. For neglecting the temporal channel variation within a single OFDM symbol, ν_{Dmax} is assumed to be much smaller than the normalized subcarrier bandwidth P/N, e.g. $\nu_{\mathrm{Dmax}} N/P < 0.01$. Under this assumption, we represent the time-variant MIMO channel by the $N \times 1$ vector $\boldsymbol{g}_{k,q}[m] = \boldsymbol{F}[h_{k,1,q}[mP, 0], \ldots, h_{k,1,q}[mP, L - 1]]^{\mathrm{T}}$. The truncated DFT matrix $\boldsymbol{F} \in \mathbb{C}^{N \times L}$ has elements $[\boldsymbol{F}]_{i,\ell} = \frac{1}{\sqrt{N}} \mathrm{e}^{\frac{-\mathrm{j}2\pi i \ell}{N}}$ for $i \in \{0, \ldots, N - 1\}$ and $\ell \in \{0, \ldots, L - 1\}$. The received signal at the qth antenna element after cyclic prefix removal and DFT is

$$\boldsymbol{y}_q[m] = \sum_{k=1}^{K} \mathrm{diag}(\boldsymbol{g}_{k,q}[m]) \boldsymbol{d}_k[m] + \boldsymbol{v}_q[m] \tag{1.35}$$

where complex additive white Gaussian noise with zero mean and covariance $\sigma_v^2 \boldsymbol{I}_N$ is denoted by $\boldsymbol{v}_q[m] \in \mathbb{C}^N$ with elements $v_q[m, e]$. We define the time-

variant effective spreading sequences

$$\tilde{\boldsymbol{s}}_{k,q}[m] = \mathrm{diag}\left(\boldsymbol{g}_{k,q}[m]\right)\boldsymbol{s}_k\,, \tag{1.36}$$

and the time-variant effective spreading matrix $\tilde{\boldsymbol{S}}_q[m] = [\tilde{\boldsymbol{s}}_{1,q}[m],\ldots,\tilde{\boldsymbol{s}}_{K,q}[m]] \in \mathbb{C}^{N\times K}$. Using these definitions, we write the signal model for data detection as

$$\boldsymbol{y}_q[m] = \tilde{\boldsymbol{S}}_q[m]\boldsymbol{a}[m] + \boldsymbol{v}_q[m] \quad\text{for}\quad m \notin \mathcal{P} \tag{1.37}$$

where $\boldsymbol{a}[m] = [a_1[m],\ldots,a_K[m]]^{\mathrm{T}} \in \mathbb{C}^K$ contains the stacked data symbols for K users. Equation (1.37) is identical to the signal model for CDMA in a frequency-flat fading environment. Thus, we apply the PIC and MMSE multiuser detection algorithms defined in Sect. 1.4.3 with ISI length $W = 1$ (cf. (1.16)). However, the effective spreading sequence (1.36) is time-variant and (1.24) must be calculated for every symbol, now.

The performance of the iterative receiver crucially depends on the accuracy with which the time-variant frequency response $\boldsymbol{g}_{k,q}[m]$ is estimated, since the effective spreading sequence (1.36) directly depends on the actual channel realizations. The MIMO-OFDM signal model (1.35) describes a transmission over $N \times N_{\mathrm{R}}$ parallel frequency-flat channels. Therefore, we rewrite (1.35) as a set of equations for every subcarrier $e \in \{0,\ldots,N-1\}$ and receive antenna $q \in \{1,\ldots,N_{\mathrm{R}}\}$,

$$y_q[m,e] = \sum_{k=1}^{K} g_{k,q}[m,e]d_{k,q}[m,e] + v_q[m,e]\,, \tag{1.38}$$

where $d_k[m,e] = s_k[e]a_k[m] + p_k[m,e]$. The temporal variation of each subcarrier coefficient $g_{k,q}[m,e]$ is bandlimited by the normalized maximum Doppler bandwidth ν_{Dmax}. We estimate $g_{k,q}[m,e]$ for an interval with length M using the received sequence $y_q[m,e]$. Slepian [24] analyzed discrete prolate spheroidal (DPS) sequences that are maximally concentrated in a given time interval and to a given bandwidth. Thus, the properties of these DPS sequences are directly relevant to the channel estimation problem. The DPS sequences are *doubly* orthogonal over the intervals $[-\infty,\infty]$ and $[0,M-1]$. We use the DPS sequences on the index set $\{0,\ldots,M-1\}$ to define an orthogonal basis. The index-limited DPS sequences will be termed *Slepian sequences*.

Slepian Basis Expansion.   The Slepian basis expansion approximates the sequence $g_{k,q}[m,e]$ by a linear combination of Slepian sequences $u_i[m]$

$$g_{k,q}[m,e] \approx \tilde{g}_{k,q}[m,e] = \sum_{i=0}^{D-1} u_i[m]\psi_{k,q}[i,e]\,, \tag{1.39}$$

where $m \in \{0,\ldots,M-1\}$ and $e \in \{0,\ldots,N-1\}$. The Slepian sequences $\boldsymbol{u}_i \in \mathbb{R}^M$ with elements $u_i[m]$ are defined as the eigenvectors of the matrix

$C \in \mathbb{R}^{M \times M}$ defined as $[C]_{i,\ell} = \frac{\sin[2\pi(i-\ell)\nu_{\mathrm{Dmax}}]}{\pi(i-\ell)}$ where $i, \ell = 0, 1, \ldots, M - 1$, i.e. $Cu_i = \lambda_i u_i$. The approximate dimension of the time-concentrated and bandlimited signal space is $D = \lceil 2\nu_{\mathrm{Dmax}} M \rceil + 1$ [24, Sec. 3.3], which means that the eigenvalues λ_i rapidly decay to zero for $i > D$. In effect, (1.39) is a reduced-rank representation for time-limited parts (or snapshots) of bandlimited sequences. The mean squared error for one subcarrier is defined as (where we omit k, q and e)

$$\mathrm{MSE}_M = \frac{1}{M} \sum_{m=0}^{M-1} \mathbb{E}\left\{ |g[m] - \tilde{g}[m]|^2 \right\} \tag{1.40}$$

The mean squared error of the Slepian basis expansion is given by the sum of two terms $\mathrm{MSE}_M = \mathrm{bias}_M + \mathrm{var}_M$. The autocorrelation of the subcarrier determines bias_M and this term decreases with growing dimension D of the basis expansion. On the other hand, var_M is proportional to D and the noise variance σ_v^2 [23]. An analytic expression for bias_M can be found in [21, 34]

$$\mathrm{bias}_M = \frac{1}{M} \sum_{m=0}^{M-1} \int_{-1/2}^{1/2} E(m, \nu) S_{gg}(\nu) \, \mathrm{d}\nu \tag{1.41}$$

where $S_{gg}(\nu)$ is the power spectral density of the subcarrier and

$$E(m, \nu) = \left| 1 - f^{\mathrm{T}}[m] G^{-1} \sum_{\ell=0}^{M-1} f^*[\ell] \, \mathrm{e}^{-\mathrm{j}2\pi\nu(m-\ell)} \right|^2, \tag{1.42}$$

with $G = \sum_{m=0}^{M-1} f[m] f^{\mathrm{H}}[m]$ and $f[m] = [u_0[m], \ldots, u_{D-1}[m]]^{\mathrm{T}} \in \mathbb{C}^D$. The variance is independent of the selected basis, $\mathrm{var}_M \approx \sigma_v^2 D / M$. The use of the Slepian basis offers a significantly smaller bias compared to the Fourier basis (i.e. the truncated discrete Fourier transform). This was demonstrated numerically and analytically in [31, 34].

We emphasize that the selection of a suitable Slepian basis, parameterized by M and ν_{Dmax}, exploits the band-limitation of the Doppler spectrum to ν_{Dmax} only. The details of the Doppler spectrum for $|\nu| < \nu_{\mathrm{Dmax}}$ are irrelevant. Our approach therefore differs from a Karhunen-Loève transform which requires *complete* knowledge of the second-order statistics of the fading process. This approach was chosen since MIMO channel sounder measurements have shown that wireless fading channels show stationary behavior for less than 70 wavelengths in a pedestrian typical urban environment [28]. We fear that meaningful short-term fading characteristics (second-order statistics, to begin with) can hardly be acquired in a multiuser MIMO system when users move at vehicular speeds.

For the purposes of performance *analysis* for a *nominal* ensemble of channel realizations, we evaluate (1.41) for a *nominal* Doppler spectrum $S_{gg}(\nu)$.

Signal Model for Time-Variant Channel Estimation. We insert the basis expansion (1.39) for the coefficients $g_{k,q}[m, e]$ in (1.38),

$$y_q[m, e] = \sum_{k=1}^{K} \sum_{i=0}^{D-1} u_i[m]\psi_{k,q}[i, e]d_k[m, e] + v_q[m, e] \,. \tag{1.43}$$

Thus, an estimate of the subcarrier coefficients $\hat{\psi}_{k,q}[i, e]$ can be obtained jointly for all K users but individually for every subcarrier e and receive antenna q. We define the stacked vector $\boldsymbol{\psi}_{e,q} = \left[\boldsymbol{\psi}_{e,q,0}^{\mathrm{T}}, \ldots, \boldsymbol{\psi}_{e,q,D-1}^{\mathrm{T}} \right]^{\mathrm{T}} \in \mathbb{C}^{KD}$ containing the basis expansion coefficients of all K users for subcarrier e where $\boldsymbol{\psi}_{e,q,i} = [\psi_{1,q}[i, e], \ldots, \psi_{K,q}[i, e]]^{\mathrm{T}} \in \mathbb{C}^{K}$. Furthermore we introduce the notation $\boldsymbol{y}_{e,q} = [y_q[0, e], \ldots, y_q[M-1, e]]^{\mathrm{T}} \in \mathbb{C}^{M}$ for the received chip sequence for a single data block on subcarrier e. Using these definitions, we write

$$\boldsymbol{y}_{e,q} = \boldsymbol{\mathcal{D}}_e \boldsymbol{\psi}_{e,q} + \boldsymbol{v}_{e,q} \,, \tag{1.44}$$

where

$$\boldsymbol{\mathcal{D}}_e = [\mathrm{diag}\,(\boldsymbol{u}_0)\,\boldsymbol{D}_e, \ldots, \mathrm{diag}\,(\boldsymbol{u}_{D-1})\,\boldsymbol{D}_e] \in \mathbb{C}^{M \times KD} \,, \tag{1.45}$$

$$\boldsymbol{D}_e = \begin{bmatrix} d_1[0, e] & \ldots & d_K[0, e] \\ \vdots & \ddots & \vdots \\ d_1[M-1, e] & \ldots & d_K[M-1, e] \end{bmatrix} \in \mathbb{C}^{M \times K} \,. \tag{1.46}$$

contains the transmitted symbols for all K users on subcarrier e. For channel estimation, the J pilot symbols in (1.34) are used. The remaining $M - J$ symbols are not known; we replace them by soft decisions that are calculated from the APP obtained in the previous iteration. This enables a refinement of the channel estimates when the soft decisions gain reliability from these iterations. For the first iteration, the soft decisions $\tilde{a}_k'[m]$ are set to zero. We define the soft decision matrix $\tilde{\boldsymbol{D}}_e \in \mathbb{C}^{M \times K}$ according to (1.46) by replacing $d_k[m, e]$ with $\tilde{d}_k[m, e] = s_k[e]\tilde{a}_k[m] + p_k[m, e]$. Finally we define $\tilde{\boldsymbol{\mathcal{D}}}_e \in \mathbb{C}^{M \times KD}$ according to (1.45) by replacing $\boldsymbol{D}_e$ with $\tilde{\boldsymbol{D}}_e$. Thus, $\tilde{\boldsymbol{\mathcal{D}}}_e$ contains *a priori* known pilot symbols and soft decisions for the unknown data symbols.

LMMSE Channel Estimation. We use the minimum mean square error (MMSE) criterion for estimating the basis expansion coefficients $\boldsymbol{\psi}_{e,q}$ (see [32] for the block fading single input single output case):

$$\hat{\boldsymbol{\psi}}_{e,q} = \left(\tilde{\boldsymbol{\mathcal{D}}}_e^{\mathrm{H}} \boldsymbol{\Delta}^{-1} \tilde{\boldsymbol{\mathcal{D}}}_e + \boldsymbol{I}_K \right)^{-1} \tilde{\boldsymbol{\mathcal{D}}}_e^{\mathrm{H}} \boldsymbol{\Delta}^{-1} \boldsymbol{y}_{e,q} \tag{1.47}$$

where $\boldsymbol{\Delta} = \boldsymbol{\Lambda} + \sigma_v^2 \boldsymbol{I}_M$. The elements of the diagonal matrix $\boldsymbol{\Lambda}$ are defined as

$$[\boldsymbol{\Lambda}]_{m,m} = \frac{1}{N} \sum_{k=1}^{K} \sum_{i=0}^{D-1} u_i^2[m] \, \mathrm{var}\{a_k[m]\}, \tag{1.48}$$

and the symbol variance is $\mathrm{var}\{a_k[m]\} = 1 - \tilde{a}_k^2[m]$. The rows of $\tilde{\boldsymbol{\mathcal{D}}}_e$ are scaled by the elements of the diagonal matrix $\boldsymbol{\Delta}$, taking into account the variances of the noise and of the soft decisions. After $\hat{\boldsymbol{\psi}}_{e,q}$ is evaluated for all $e \in \{0, \ldots, N-1\}$ and $q \in \{1, \ldots, N_\mathrm{R}\}$, an estimate for the time-variant frequency response is given by $\hat{g}_{k,q}[m,e] = \sum_{i=0}^{D-1} u_i[m] \hat{\psi}_{k,q}[i,e]$. Additional noise suppression is obtained if we exploit the correlation between the subcarriers $\hat{\boldsymbol{g}}_{k,q}[m] = \boldsymbol{F}\boldsymbol{F}^\mathrm{H}\hat{\boldsymbol{g}}_{k,q}[m]$. Finally, the data is detected by inserting the channel estimates $\hat{\boldsymbol{g}}_{k,q}[m]$ into (1.36).

Simulation Results and Discussion. Realizations of the time-variant frequency-selective MIMO channel $h_{k,1,q}[n,\ell]$ are generated using an exponentially decaying power-delay profile (PDP) $\eta^2[\ell] = \mathrm{e}^{-\ell/4}/\sum_{\ell'=0}^{L-1} \mathrm{e}^{-\ell'/4}$, $\ell = 0, \ldots, L-1$, [10] with essential support of $L = 15$. The time indices n and ℓ correspond to sampling at rate $1/T_\mathrm{C}$. The PDP corresponds to a root mean square delay spread $T_\mathrm{D} = 4T_\mathrm{C} = 1\mu\mathrm{s}$ for a chip rate of $1/T_\mathrm{C} = 3.84 \cdot 10^6 \, 1/\mathrm{s}$. The autocorrelation for every channel tap is given by $R_{h'h'}[n,\ell] = \eta^2[\ell]J_0(2\pi\nu_\mathrm{D}Pn)$ which results in the classical Jakes' spectrum. We simulate the time-variant channel using the model in [35] corrected for low velocities in [33].

The system operates at carrier frequency $f_\mathrm{C} = 2\,\mathrm{GHz}$ and the $K = 64$ users move with velocity $v \in \{0, 100\}\,\mathrm{km/h}$. This gives a Doppler bandwidth of $B_\mathrm{D} = 190\,\mathrm{Hz}$ corresponding to $\nu_\mathrm{D} = 0.0039$. The number of subcarriers is $N = 64$ and the length of the OFDM symbol with cyclic prefix is $P = G + N = 79$. The data block consists of $M = 256$ OFDM symbols with $J = 60$ OFDM pilot symbols. The system is designed for a maximum velocity $v_\mathrm{max} = 100\,\mathrm{km/h}$ which results in $D = 3$ for the Slepian basis expansion. The base station uses $N_\mathrm{R} \in \{1, 2, 4\}$ receive antennas. All simulation results are averaged over 100 independently generated data blocks.

In Fig. 1.6, we illustrate the multiuser MIMO-OFDM uplink performance with iterative time-variant channel estimation based on the Slepian basis expansion in terms of bit error rate (BER) versus E_b/N_0 after 4 iterations. We also display the single-user bound (SUB) which is defined as the BER for one user and perfect channel knowledge at the receiver, as well as the "basis expansion SUB" which is the achievable BER with a channel estimation scheme based on the Slepian basis expansion. With increasing number of coherently combined receive antennas, the channel estimation variance described by var_M becomes the limiting factor for the receiver performance.

Simulation results show that an iterative receiver using the Slepian basis expansion for channel equalization handles a wide range of user velocities
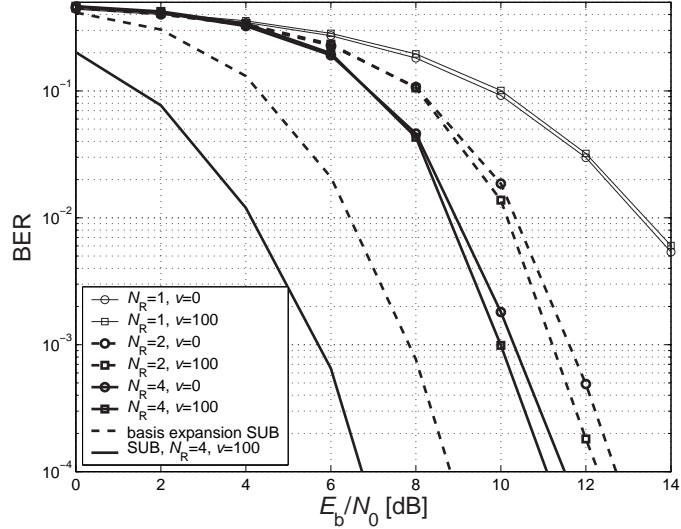
Fig. 1.6   BER versus SNR on the uplink for multiuser MIMO-OFDM after 4 iterations and Slepian basis expansion for $D = 3$, $K = 64$ users are static ($v = 0\,\text{km/h}$) or moving at $v = 100\,\text{km/h}$, receiver employs $N_\text{R} = 1$, 2, or 4 antennas.

under full load. Accurate channel estimates obtained with the Slepian basis expansion with soft decisions allow to exploit the Doppler diversity. This leads to *decreased* BER at higher velocities.

REFERENCES

1. P.D. Alexander, A.J. Grant, and M.C. Reed. Iterative detection in code-division multiple-access with error control coding. *European Transactions on Telecommunications*, 1998.

2. H. Artés and F. Hlawatsch. Blind equalization of MIMO channels using deterministic precoding. In *Proc. IEEE ICASSP'01*, pages 2153–2156, Salt Lake City (UT), USA, May 2001.

3. H. Artés and F. Hlawatsch. Space-time matrix modulation: Rank-deficient channels and multi-user case. In *Proc. IEEE ICASSP'02*, pages 2225–2228, Orlando (FL), USA, May 2002.

4. L.R. Bahl, J. Cocke, F. Jelinek, and J. Raviv. Optimal decoding of linear codes for minimizing symbol error rate. *IEEE Transactions on Information Theory*, pages 284–287, March 1974.

5. J. Baltersee, G. Fock, and H. Meyr. Achievable rate of MIMO channels with data-aided channel estimation and perfect interleaving. *IEEE Journal on Selected Areas in Communications*, 19(12):2358–2368, December 2001.

6. J. Boutros and G. Caire. Iterative multiuser joint decoding: Unified framework and asymptotic analysis. *IEEE Transactions on Information Theory*, 48(7):1772–1793, July 2002.

7. J.J. Boutros, F. Boixadera, and C. Lamy. Bit-interleaved coded modulations for multiple input multiple-output channels. In *Proc. IEEE Symp. Spread Spectrum Techn. Appl. (ISSSTA'00)*, pages 123–126, Parsippany (NJ), USA, September 2000.

8. G. Caire and U. Mitra. Structured multiuser channel estimation for block-synchronous DS/CDMA. *IEEE Transactions on Communications*, 49(9):1605–1617, September 2001.

9. G. Caire and R.R. Müller. The optimal received power distribution for IC-based iterative multiuser joint decoders. In *Proc. 39th Annual Allerton Conf. on Comm., Cont., and Comp.*, Monticello, IL, USA, October 2001.

10. L.M. Correia. *Wireless Flexible Personalised Communications*. Wiley, 2001.

11. B. Hochwald and T. Marzetta. Unitary space-time modulation for multiple-antenna communications in Rayleigh flat fading. *IEEE Transactions on Information Theory*, 46:543–564, March 2000.

12. B. Hochwald and W. Sweldens. Differential unitary space-time modulation. *IEEE Transactions on Communications*, 48:2041–2052, December 2000.

13. B.L. Hughes. Differential space-time modulation. *IEEE Transactions on Information Theory*, 46:2567–2578, November 2000.

14. M. Kobayashi, J. Boutros, and G. Caire. Successive interference cancellation with SISO decoding and EM channel estimation. *IEEE Transactions on Communications*, 19(8):1450–1460, August 2001.

15. Y. Li and L.J. Cimini. Bounds on the interchannel interference of OFDM in time-varying impairments. *IEEE Transactions on Communications*, 49(3):401–404, March 2001.

16. M. Loncar, R.R. Müller, J. Wehinger, and T. Abe. Iterative joint detection, decoding and channel estimation for dual antenna arrays in frequency selective fading. In *Proc. URSI 2002*, Maastricht, The Netherlands, August 2002.

17. M. Medard. The effect upon channel capacity in wireless communications of perfect and imperfect knowledge of the channel. *IEEE Transactions on Information Theory*, 46:933–946, May 2000.

18. A. Medles and D.T.M. Slock. Semiblind channel estimation for MIMO spatial multiplexing systems. In *Proc. IEEE VTC'01*, volume 2, pages 1240–1244, 2001.

19. M. Moher. An iterative multiuser decoder for near-capacity communications. *IEEE Transactions on Communications*, 46(7):870–880, July 1998.

20. T.J. Moore, B.M. Sadler, and R.J. Kozick. Regularity and strict identifiability in MIMO systems. *IEEE Transactions on Signal Processing*, 50(8):1831–1842, August 2002.

21. M. Niedzwiecki. *Identification of Time-varying Processes*. John Wiley & Sons, Ltd., 2000.

22. A.M. Sayeed, A. Sendonaris, and B. Aazhang. Multiuser detection in fast-fading multipath environment. *IEEE Journal on Selected Areas in Communications*, 16(9):1691–1701, December 1998.

23. L.L. Scharf and D.W. Tufts. Rank reduction for modeling stationary signals. *IEEE Transactions on Acoustics, Speech, and Signal Processing*, ASSP-35(3):350–355, March 1987.

24. D. Slepian. Prolate spheroidal wave functions, Fourier analysis, and uncertainty - V: The discrete case. *The Bell System Technical Journal*, 57(5):1371–1430, May-June 1978.

25. Q. Sun, D.C. Cox, H.C. Huang, and A. Lozano. Estimation of continuous flat fading MIMO channels. *IEEE Transactions on Wireless Communications*, 1(4):549–553, October 2002.

26. A.L. Swindlehurst and G. Leus. Blind and semi-blind equalization for generalized space-time block codes. *IEEE Transactions on Signal Processing*, 50(10):2489–2498, October 2002.

27. M. Tüchler, R. Koetter, and A.C Singer. Turbo equalization: Principles and new results. *IEEE Transactions on Communications*, 50(5):754–767, May 2002.

28. I. Viering and H. Hofstetter. Potential of coefficient reduction in delay, space and time based on measurements. In *37th Conference on Information Sciences and Systems (CISS 2003)*, John Hopkins University, March 2003.

29. X. Wang and H.V. Poor. Iterative (turbo) soft interference cancellation and decoding for coded CDMA. *IEEE Transactions on Communications*, 47(7):1046–1061, July 1999.

30. J. Wehinger, R.R. Müller, M. Lončar, and C.F. Mecklenbräuker. Performance of iterative CDMA receivers with channel estimation in multipath environments. In *Proc. Asilomar Conf. on Signals, Systems and Computers*, Pacific Grove (CA), USA, November 2002.

31. T. Zemen. *OFDM Multi-User Communication Over Time-Variant Channels, Doctoral Thesis*. Vienna University of Technology, Vienna, Austria, August 2004.

32. T. Zemen, M. Lončar, J. Wehinger, C.F. Mecklenbräuker, and R.R. Müller. Improved channel estimation for iterative receivers. In *IEEE Global Telecommunications Conference, GLOBECOM'03*, volume 1, pages 257–261, San Francisco (CA), USA, December 2003.

33. T. Zemen and C.F. Mecklenbräuker. Doppler diversity in MC-CDMA using the Slepian basis expansion model. In *12th European Signal Processing Conference (EUSIPCO)*, Vienna, Austria, September 2004.

34. T. Zemen and C.F. Mecklenbräuker. Time-variant channel estimation for MC-CDMA using prolate spheroidal sequences. *IEEE Transactions on Signal Processing*, 53, 2005. to appear.

35. Y.R. Zheng and C. Xiao. Simulation models with correct statistical properties for Rayleigh fading channels. *IEEE Transactions on Communications*, 51(6):920–928, June 2003.

Index